Acclerated microwave processing of nanocrystalline hydroxyapatite

N. RAMESHBABU
Department of Metallurgical and Materials Engineering, Indian Institute of Technology Madras, Chennai 600036, India; Sophisticated Analytical Instrument Facility, Indian Institute of Technology Madras, Chennai 600036, India

K. PRASAD RAO
Department of Metallurgical and Materials Engineering, Indian Institute of Technology Madras, Chennai 600036, India

T. S. SAMPATH KUMAR*
Department of Metallurgical and Materials Engineering, Indian Institute of Technology Madras, Chennai 600036, India; Sophisticated Analytical Instrument Facility, Indian Institute of Technology Madras, Chennai 600036, India
E-mail: tssk@iitm.ac.in

Published online: 1 November 2005

Hydroxyapatite is a major mineral component of the calcified tissues (i.e. bones and teeth). Synthetic hydroxyapatite (HA, $Ca_{10}(PO_4)_6(OH)_2$) has been extensively used as an implant material for bone substitute owing to its excellent osteoconductive properties [1]. Synthetic HA has been used for a variety of other biomedical applications like matrices for controlled drug release, bone cements, tooth paste additive, dental implants etc [2–5]. Non-medical applications of HA include packing media for column chromatography, gas sensors, catalysis and host materials for lasers [6]. These applications stimulate to develop new methods to synthesis HA. The preparation of nanocrystalline HA is of paramount importance as the large surface area of the diminutive crystals makes them very active and consequently affects strongly the properties of the solids produced from them. Cell proliferation, synthesis of alkaline phosphatase and deposition of calcium-containing mineral was significantly greater by osteoblasts cultured on nanophase (grain size 67 nm) HA than the conventional HA (grain size 179 nm) [7]. Nanophase HA can be synthesized by several routes such as co-precipitation process using calcium nitrate and phosphoric acid, mechano-chemical reaction, precipitation using emulsion, template and sol–gel techniques [8–12]. However to obtain nano-HA these methods need highly controlled parameters such as reactant concentrations, pH, temperature of the aqueous solutions and 24–50 hr of processing time. Nanocrystalline HA particles of about 300 nm on edges were precipitated by submitting calcium chloride and sodium phosphate solutions to microwave irradiation followed by quenching in ice [13]. The chloride ion with radius of $r_{Cl^-}=181$ pm may enter the crystal lattice of HA substituting hydroxyl groups ($r_{OH^-}=151$ pm) and sodium ions may also substitute the calcium ions ($r_{Ca^{2+}} = 99$ pm, $r_{Na^+} = 95$ pm) leading to the formation of non-stoichiometric HA [14].

The main objective of the present work is to synthesize pure HA nanocrystals in a rapid way by microwave processing using suitable starting materials to avoid unnecessary substitutions. The selected materials will also maintain required pH conditions (pH > 9.0) for the synthesis of HA with out any ammonium hydroxide addition, which is generally added to maintain necessary pH condition to avoid calcium deficient apatite formation with other precursor materials.

Analytical grade calcium hydroxide ($Ca(OH)_2$, E. Merck, Germany) and di-ammonium hydrogen phosphate (DAP, $(NH_4)_2HPO_4$, E. Merck, Germany) were used for the preparation of HA nanoparticles. The amount of the reactants was calculated based on the Ca/P molar ratio of 10/6. The 0.4 M DAP solution was added to the 0.5 M calcium hydroxide suspension in 1 min under high-speed stirring conditions. This solution with a pH of 11 (Thermo Orion 420A, USA) was immediately subjected to the microwave irradiation for about 15 min in a domestic microwave oven (BPL India, 2.45 GHz, 800 W power). The mixing, crystallization of the HA and its aging occurs under the microwave irradiation in a shorter period. The product obtained after filtration was oven-dried at 70 °C for overnight and the cake obtained after drying was powdered with agate mortar and pestle. A solution with the same concentration of the above reactants was also heated at 100 °C for 20 min in a water bath to stimulate the precipitation reaction for comparison with microwave processing. Depending upon the applications, nano-HA powders can be used directly in the as synthesized condition or highly crystalline heat treated condition or sintered compacts for different biomedical applications. Thermal stability of the HA powder is also important for coating metallic implants which usually involves a post-coating heat treatment at 800–900 °C [15]. To examine the thermal stability of the HA, a small amount of the sample was heated at 1000 °C for 2 hr. The oven dried and 1000 °C heated samples

* Author to whom all correspondence should be addressed.

0022-2461
DOI: 10.1007/s10853-005-2957-9

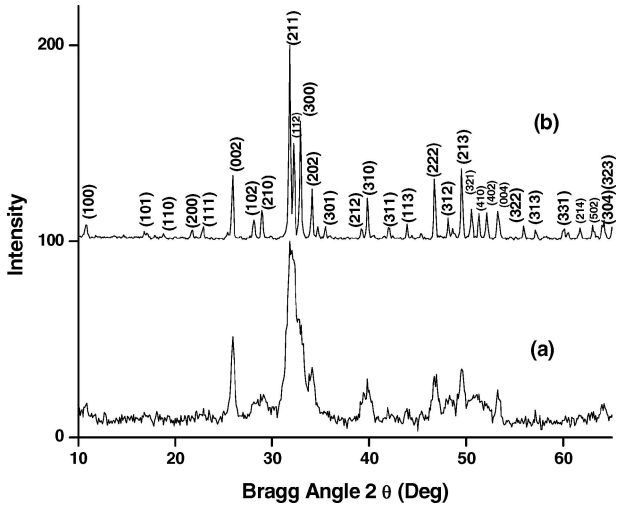

Figure 1 XRD patterns of oven-dried (a) and 1000 °C heated (b) HA nanoparticles.

were characterized by X-ray diffraction (XRD) method (Shimadzu, XD-D1, Japan). The functional groups present in HA were ascertained by Fourier transform infrared spectroscopy (FT-IR) and Fourier transform Raman spectroscopy (FT-Raman) methods (Bruker, IFS 66V FT-IR spectrometer, Germany equipped with FRA 106 Raman module). The FT-IR and FT-Raman spectra (Nd:YAG laser, 1064 nm wavelength) were obtained in the region of 450–4000 cm^{-1} and 50–3500 cm^{-1} with the spectral resolution of 4 cm^{-1}. The HA size and morphology were examined using a transmission electron microscope (TEM, CM12 STEM, Netherlands). A typical XRD pattern of the oven-dried HA sample is shown in Fig. 1. The XRD peaks were markedly broader, which suggested that HA particles were nanosized. The diffraction peaks of the heat treated HA are well resolved as shown in Fig. 1 and correspond to the hexagonal hydroxyapatite crystal (JCPDS 9-432). The presence of other calcium phosphate phases was not detected. The peak broadening of the XRD reflection was used to estimate the crystallite size in a direction perpendicular to the crystallographic plane based on Scherrer's formula. The diffraction peak at 25.9° was chosen for calculation of the crystallite size; since it is sharper and isolated form others. This peak assigns to (0 0 2) Miller's plane family and shows the crystal growth along the *c*-axis of the HA crystalline structure. The estimated crystallite sizes were 28 and 56 nm for the oven-dried and 1000 °C heated samples respectively. The reaction kinetics of HA precipitation seems to be enhanced under microwave irradiation leading to nanocrystalline material. The HA powder heat treated at 1000 °C does not show any secondary phase formation (e.g., tricalcium phosphate or calcium oxide), indicating its thermal stability with marked improvement in crystallinity by narrowing of the diffraction lines. The thermal stability of the HA powder in the present study may be due to its Ca/P ratio being closer to the stoichiometric ratio of 10/6. The *a*-axis expands from 9.398 to 9.411 Å on heating from 70 °C to 1000 °C whereas the change along *c*-axis is negligible (6.883 to 6.881 Å). Although the JCPDS value for HA is 9.418 Å, similar low value of *a*-axis has been reported for nanophase HA [11]. The fraction of crystalline phase (X_c) in HA powder has been calculated by the following equation:

$$X_c \approx 1 - (V_{112/300})/I_{300}) \quad (1)$$

where I_{300} is the intensity of the (300) diffraction peak and $V_{112/300}$ is the intensity of the hollow between (112) and (300) diffraction peaks [16]. The X_C increases from 8 to 97% for the oven-dried and 1000 °C heated HA powders respectively.

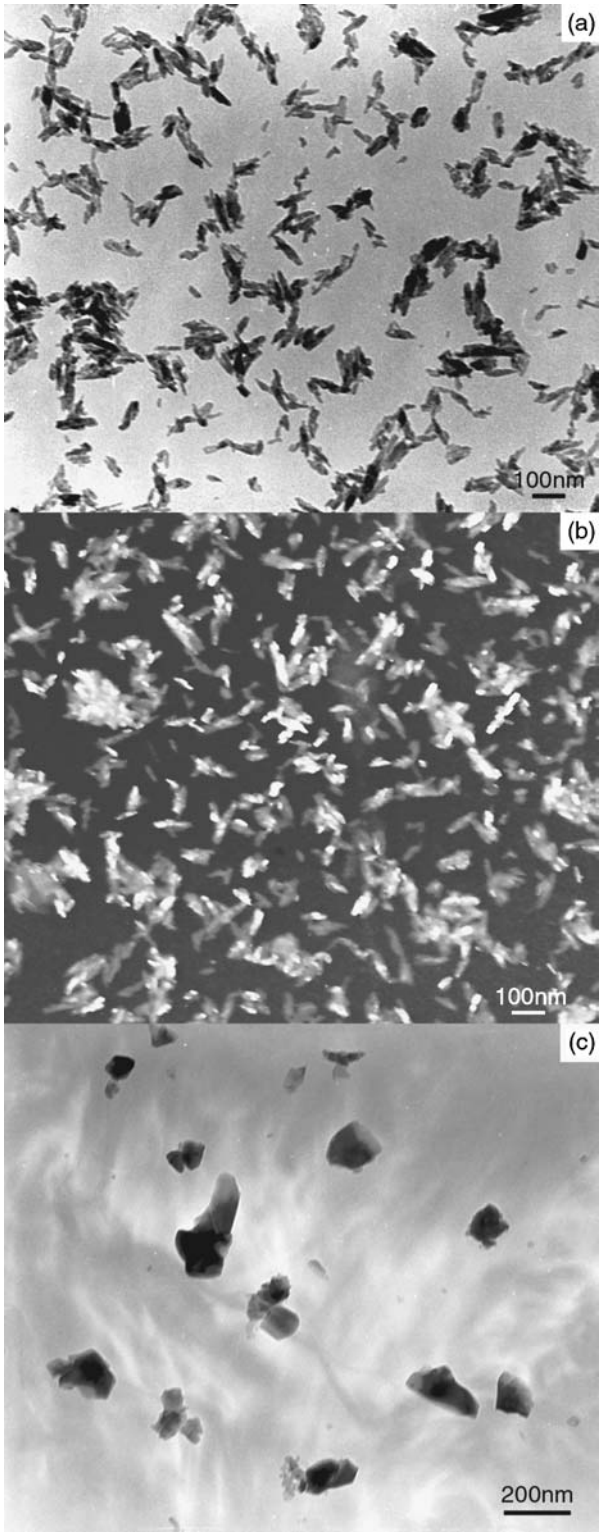

Figure 2 TEM bright field image (a), dark field image (b) of oven-dried HA nanoparticles and bright field image of 1000 °C heated HA (c).

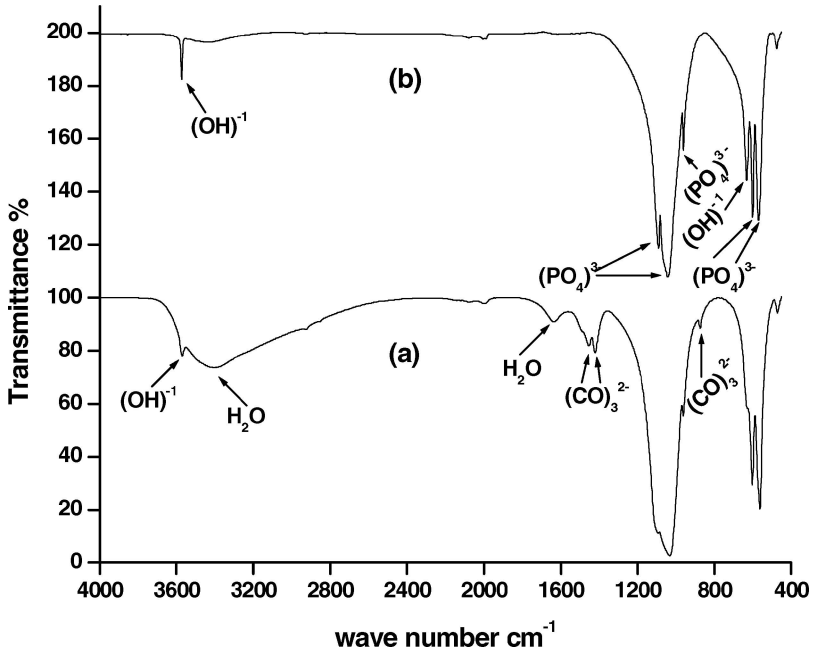

Figure 3 FT-IR spectra of oven-dried (a) and 1000 °C heated (b) HA nanoparticles.

Both the bright and dark field transmission electron microscope images of the oven-dried HA particles are shown in Fig. 2a and b respectively. The oven dried HA particles were of nano-plate like morphology with 15–20 nm width and 60–80 nm length respectively. The particles were a bit thinner and longer with more irregular and less clear contour. Also the particles showed high tendency to agglomerate. On the other hand for the 1000 °C heated HA (Fig. 2c), the particles were thicker and shorter with more regular and clear contours and less agglomeration. The increase of crystallinity with heating was also proved by FT-IR analysis. Fig. 3 shows the FT-IR spectra of the oven-dried and 1000 °C heated powders. The characteristic bands for HA are exhibited in both the spectra: 900–1200 cm^{-1} for phosphate bending and stretching, 602 cm^{-1} for phosphate bending, 632 cm^{-1} and 3571 cm^{-1} for librational & stretching modes of hydroxyl vibrations. The intensities of both the hydroxyl bands and the band at 962 cm^{-1} for phosphate can be used as an indication of the HA crystallinity [11]. The intensities of these bands increase with heating and this result is coincident with the above XRD results as shown in Fig. 1. In addition, the broad bands observed at 1630 and 3400 cm^{-1} due to adsorbed water in HA powder also drastically decreases with the heating. The characteristic bands corresponding to phosphate bending near 1040 and 1090 cm^{-1} were broadened and blue shifted for the oven-dried sample compared to 1000 °C heated HA sample. This may be due to the small dimension

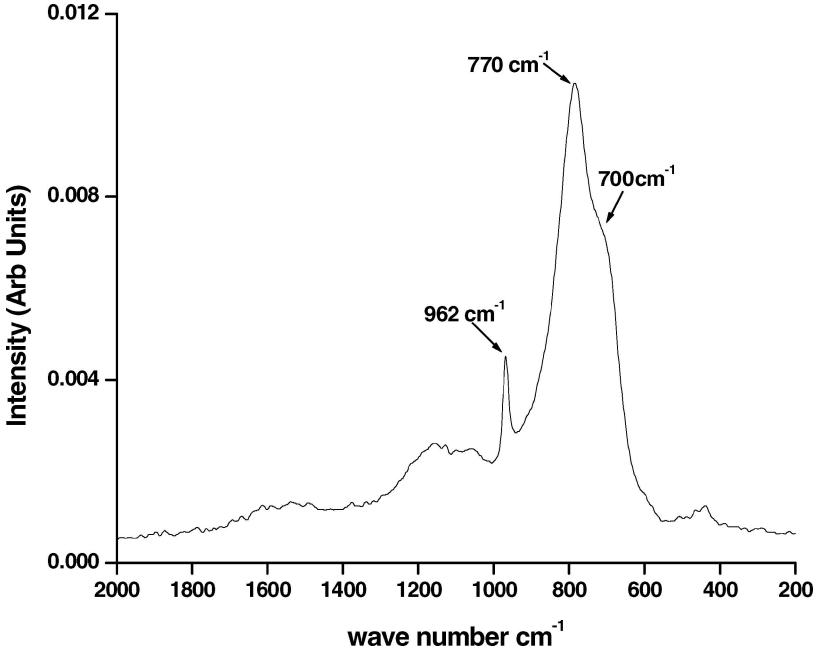

Figure 4 FT-Raman spectrum of synthesized HA nanoparticles.

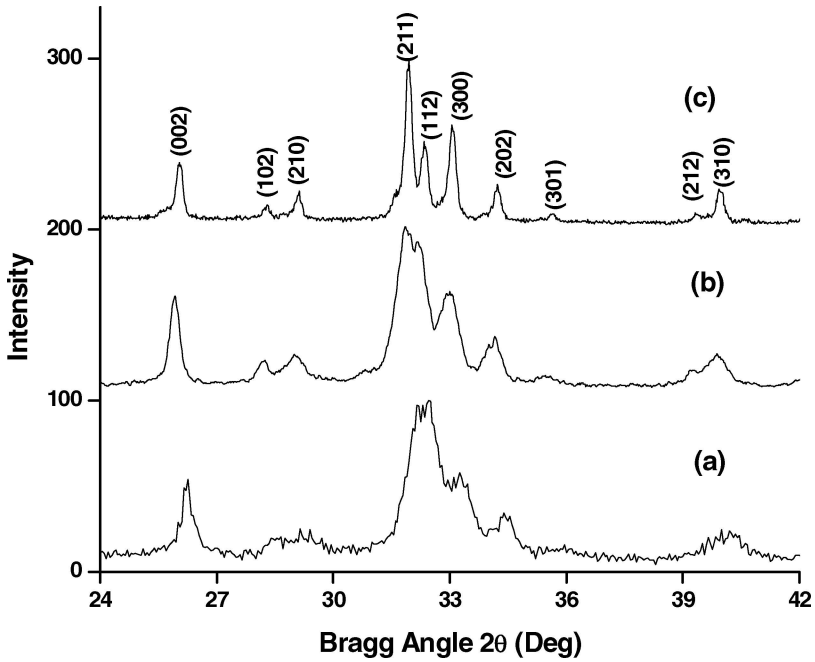

Figure 5 XRD patterns of the HA powders prepared by conventional heating at 100 °C, for 20 min (a), microwave processing for 20 min (b) and 60 min (c).

effect of HA nanoparticles [12]. The absorption bands at 873, 1421 and 1455 cm^{-1} of oven-dried samples are assigned to the presence of carbonate ions in the HA sample. The carbonate ion may come from a reaction between carbon dioxide and high solution pH [17]. However, the human bone or synthetic HA when heated above 700 °C readily lose their carbonate ions [18]. The carbonate bands were absent in 1000 °C heated sample in the present study, also due to the loss of carbonate ions during heating in air. Since, carbonate containing HA is well known to have a better bioactivity due to its similarity to the chemical composition of biological apatite in natural bone, the nano-HA obtained in the present study are expected to demonstrate good biocompatibility.

The FT-Raman spectrum of the oven-dried HA is shown in Fig. 4. In addition to the Raman line at 962 cm^{-1} for the skeletal stretching mode of phosphate, two fluorescence bands appear in the FT-Raman spectrum at 700 and 770 cm^{-1} respectively. There were no vibration modes of O–H, O–H–O bonds and other modes. As stoichiometric apatite compounds only have been reported to give rise to fluorescence bands in the FT-Raman spectra [19], the synthesized nano-HA in the present work seems to be of stoichiometric hydroxyapatite.

The XRD pattern of HA formed by the precipitation reaction for 20 min at 100 °C by conventional heating is shown in Fig. 5 for comparison with microwave processing. The HA was found be of low crystallanity by conventional heating. By varying the microwave power and (or) time it is also possible to synthesize nano-HA with different degrees of crystallinity. The HA prepared by varying the irradiation time for 20 and 60 min at 800 W power was found to be of medium and high crystallinity respectively as also shown in Fig. 5. In conclusion, microwave processing seems to be effective in synthesizing HA with nano-plate like morphology using simple precursors in a rapid way. The morphology of HA in the present study has been found to be different from the reported nanorods [20] or spherical irregular size particles [21] obtained by microwave processing using different precursor materials. The microwave heating reduced the HA crystallization time and improved crystallinity of the final product. The selected starting materials also found to be the ideal materials to synthesize pure and thermally stable nano-HA with out any unnecessary substitutions.

References

1. K. GROOT, *Biomaterials* **1** (1980) 47.
2. R. Z. LEGEROS, *Adv. Dent. Res.* **2** (1998) 164.
3. M. ITOKAZU, W. YANG, T. AOKI and N. KATO, *Biomaterials* **19** (1998) 817.
4. S. M. KENNY and M. BUGGY, *J. Mater. Sci. Mater. Med.* **14** (2003) 923.
5. M. NIVA, T. SATO and W. LI, *ibid.* **12** (2001) 277.
6. R. E. RIMAN, W. L. SUCHANEK, K. BYRAPPA, CHUN-WEI CHEN, P. SHUK and C. S. OAKES, *Solid State Ion.* **151** (2002) 393.
7. T. J. WEBSTER, C. ERGUN, R. A. DOREMUS, R. W. SIEGEL and R. BIZIOS, *Biomaterials* **21** (2000) 1803.
8. L. B. KONG, J. MA and F. BOEY, *J. Mater. Sci.* **37** (2002) 1131.
9. K. C. B. YEONG, Y. WANG and S. C. NG, *Biomaterials* **22** (2001) 2705.
10. K. SONODA, T. FURUZONO, D. WALSH, K. SATO and J. TANAKA, *Solid State Ion.* **151** (2002) 321.
11. R. N. PANDA, M. F. HSIECH, R. J. CHUNG and T. S. CHIN, *J. Phys. Chem. Solids* **62** (2003) 193.
12. Y. ZHANG, L. ZHOU, D. LI, N. XUE, X. XU and J. LI, *Chem. Phys. Lett.* **376** (2003) 493.
13. S. SARIG and F. KAHANA, *J. Cryst. Growth* **237** (2002) 55.
14. H. HOHL, P. G. KOUTSOUKOS and G. H. NANCOLLAS, *ibid.* **57** (1982) 325.
15. B. MAVIS and A. C. TAS, *J. Amer. Ceram. Soc.* **83** (2000) 989.

16. E. LANDI, A. TAMPIERI, G. CELOTTI and S. SPRI, *J. Eur. Ceram. Soc.* **20** (2000) 2377.
17. P. N. KUMTA, C. SFEIR, DONG-HYUN LEE, D. OLTON and D. CHOI, *Acta. Biomaterialia* **1** (2005) 73.
18. S. JALOTA, A. C. TAS and S. B. BHADURI, *J. Mater. Res.* **19** (2004) 1879.
19. A. HADRICH, A. LAUTIE and T. MHIRI, *Spectra. Chem. Acta* **A57** (2001) 1673.
20. J. LIU, K. LI, H. WANG, M. ZHU and H. YAN, *Chem. Phys. Lett.* **396** (2004) 430.
21. P. PARHI, A. RAMANAN and A. R. RAY, *Mater. Lett.* **58** (2004) 3611.

Received 17 September 2004
and accepted 13 June 2005